ACS APPLIED MATERIALS & INTERFACES

Energy, Environmental, and Catalysis Applications

Activation energy of hydrogen adsorption on Pt(111) in alkaline media: an impedance spectroscopy study at variable temperatures

Luis Enrique Botello, Juan Miguel Feliu, and Victor Climent

ACS Appl. Mater. Interfaces, **Just Accepted Manuscript** • DOI: 10.1021/acsami.0c13158 • Publication Date (Web): 24 Aug 2020

Activation Energy of Hydrogen Adsorption on Pt(111) in Alkaline Media: an Impedance Spectroscopy Study at Variable Temperatures

Luis E. Botello, Juan M. Feliu, and Victor Climent*

Instituto Universitario de Electroquimica, Universidad de Alicante, Carretera San Vicente del Raspeig s/n, E-03690 San Vicente del Raspeig, Alicante, Spain

E-mail: victor.climent@ua.es

Phone: +34 965903400 x 2794

Abstract

The hydrogen evolution reaction is one of the most studied processes in electrochemistry and platinum is by far the best catalyst for this reaction. Despite the importance of this reaction on platinum, detailed and accurate kinetic measurements of the steps that lead to the main reaction are still lacking, particularly because of the fast rate of the reaction. Hydrogen adsorption on Pt(111) has been taken as a benchmark system in a large number of computational studies but reliable experimental data to compare with the computational studies is very scarce. To gain further knowledge on this matter, a temperature study of the hydrogen adsorption reaction has been carried out to obtain kinetic information for this process on Pt(111), in alkaline solution. This was achieved by measuring electrochemical impedance spectra and cyclic voltammograms in the range of $278 \leq T \leq 318$ (K), to obtain the corresponding surface coverage by adsorbed species and the faradaic charge transfer resistance. From this data, the standard rate constant has been extracted with a kinetic model assuming a Frumkin type

isotherm, resulting in values of $2.60 \times 10^{-7} \leq k^0 \leq 1.68 \times 10^{-6}$ (s^{-1}) respectively. The Arrehnius plot gives an activation energy of $32\, kJ\, mol^{-1}$. Comparisons are made with reported values for the overall HER and those calculated by computational methods, giving a reference frame to support future studies on hydrogen catalysis.

Keywords

Hydrogen, Adsorption, Electrochemistry, Activation Energy, Impedance, Platinum, Single Crystal, Akaline Media

1 Introduction

The implementation of modern strategies towards a clean and sustainable energy model on a global scale depends highly on the use of hydrogen as an energy vector.[1–3] This has motivated intensive research into the processes related with H_2 production[4] and storage.[5] In this context, the hydrogen evolution reaction (HER) is of great interest, both to the applied and fundamental body of scientific knowledge. Thus, a large variety of electrochemical and non-electrochemical tools have been applied for its study.[6] For this reaction, platinum is the most efficient pure metal, its activity only surpassed by some bimetallic alloys.[7–9] In this context, studies with single crystal platinum electrodes are valuable to elucidate the details of the reaction, since the highly ordered surfaces allow the use of theoretical models to analyze the results.[10] In this regard, a large number of computational studies have taken the H−Pt(111) system as a benchmark for their calculations[11–13] For this reason, increasing the experimental information on this system by supplying reliable data to compare with computational results will be of great importance to the progress of this field. Previous publications have reported experimental values of hydrogen adsorption energies on Pt(111)[14,15] but there is a lack of kinetic data such as activation energies.

Different voltammetric techniques have been used to obtain relevant kinetic and thermo-

dynamic data on the overall HER on platinum,[14,16,17] which is accepted to be comprised, in acidic solution, by a combination of two of the following steps:[18]

$$\mathrm{Pt} + \mathrm{H^+} + \mathrm{e} \underset{k_{-1}}{\overset{k_1}{\rightleftharpoons}} \mathrm{PtH_{ads}} \tag{1}$$

$$\mathrm{PtH} + \mathrm{H^+} + \mathrm{e} \underset{k_{-2}}{\overset{k_2}{\rightleftharpoons}} \mathrm{Pt} + \mathrm{H_2} \tag{2}$$

$$2\,\mathrm{PtH} \underset{k_{-3}}{\overset{k_3}{\rightleftharpoons}} 2\,\mathrm{Pt} + \mathrm{H_2} \tag{3}$$

Here, k_i represents the rate constants of the reactions. Equation (1) is the Volmer step, (2) is the Heyrovsky step and (3) is the Tafel step. The HER is then started with an adsorption (Volmer) step which is followed by either the Heyrovsky or the Tafel step or a combination of both.[19] The corresponding steps in alkaline media involve bond breaking in the water molecule generating OH^- anions. The voltammetric techniques offer insights into the thermodynamic aspects of the Volmer step, but since the reaction is very fast, only the overall HER can be used to obtain kinetic parameters in either acidic or alkaline solutions,[20,21] accepting that the first step is so rapid that it can be considered in equilibrium. In such fast reactions, electrochemical impedance spectroscopy (EIS) has long been used to resolve the overall process into its individual contributions.[22–25] At low frequencies, the hydrogen adsorbed on the platinum surface creates a measurable capacitive behavior that disappears when the frequency is increased, leaving only a response due to the capacitive contribution of the double layer.[26] EIS measurements can be rationalised using equivalent electrical circuits to get a simpler description of the physicochemical processes involved. In the case of hydrogen adsorption, the system can be represented by the circuit presented in the inset of figure 2, where R_s represents the resistance between the working and counter electrodes and is called the solution resistance, R_{ct} is the charge transfer resistance of the faradaic process, CPE is the capacitance of the double layer (C_{dl}) expressed as a constant phase element and C_{ad} is the pseudocapacitance associated to the adlayer formation/dissolution. The relationships between the equivalent electric elements and the chemical parameters of the

reaction are given in the supporting information. This model has been used to study the kinetics of the Volmer step on acidic[27,28] and alkaline[29–31] media on platinum and other solid electrodes. The reaction is, however, too fast in acidic media, and special equipment is needed to obtain accurate kinetic data without noise or electronic artifacts at frequencies of more than 1 MHz.[32] Nevertheless, the reaction is much slower in alkaline media and this has allowed the measurement of charge transfer resistance for hydrogen adsorption in such systems.[33,34] To the best of our knowledge, there has been no attempt to measure the effect of temperature on the rate of hydrogen adsorption on well-defined surfaces. Such measurements can provide activation energies through an Arrhenius type analysis. This information is not only important from a fundamental point of view but it supplies valuable experimental data to compare or to validate an increasingly available number of theoretical studies that calculate and use this parameter for the investigation of hydrogen processes.[35–38]

2 Experimental Section

The 0.05 M working solutions were prepared from sodium hydroxide monohydrate (Merck Suprapur) and ultrapure water (Milli-Q, 18.2 MΩ cm). All glassware was cleaned with an acidic potassium permanganate solution before rinsing it and boiling with ultrapure water. The platinum single-crystal (111) working electrode with an area of $0.0523 cm^{-2}$ was prepared with the method described by Clavilier et al.[16] and a platinum wire was used as a counter electrode. Prior to every measurement, the solution was bubbled with argon during 5 min and then left under an argon atmosphere. The Pt(111) electrode was flame annealed in a propane-butane-oxygen flame and cooled in an argon-hydrogen (3:1) atmosphere. Then, it was transferred to the electrochemical cell protected by a droplet of ultrapure water saturated with the argon-hydrogen mixture. A palladium-hydrogen electrode[39] was used as a reference and it was placed directly inside of the working solution to avoid any change in the reference potential due to thermodiffusion in the electrochemical cell and to decrease

the impedance of the reference electrode that can increase the noise in the potentiostat. The electrochemical cell was bubbled with hydrogen and the equilibrium potential for the hydrogen reduction/oxidation reaction was measured using a flame annealed platinum electrode at the beginning and the end of every session, in order to monitor the stability of the reference electrode potential. This measurement was used to convert the potentials to the reversible hydrogen electrode (RHE) scale. A PolyScience refrigerated circulator was used to keep the electrochemical cell in a bath at a constant temperature that was varied in the range $278 \leq T \leq 318$ (K), with increments of $5(\pm 0.1)\, K$.

An Ivium CompactStat.e potentiostat was used to acquire the cyclic voltammograms and the impedance measurements. For every temperature, nine different potentials were studied, from 0 to 0.5 V vs. Pd/H. However, all the potentials hereafter are reported with respect to the RHE at the same temperature of the experiment. For every potential, the impedance spectrum was recorded with frequencies from 10^5 to 0.1 Hz and a 5 mV amplitude at least three times. The data was fitted using the equivalent circuit of figure 1, using the LEVMW 8.12 software.[40] At the beginning of every experiment, a blank voltammogram was measured at $50\, mV\, s^{-1}$ to assess the state of the electrode surface, then it was repeated every three potentials. After the measurement of nine spectra, the working electrode was flame annealed again. The two highest temperatures were the exception to this protocol, since the solution was more easily contaminated, and the electrode had to be flame annealed after every impedance measurement.

3 Results and discussion

Typical cyclic voltammograms recorded for the Pt(111) electrode in 0.05 M NaOH solution at the different working temperatures are shown in figure 1.

The region of H_{upd}, between $E \approx 0.05$ and 0.4 V, does not change in the recorded temperature range, except for the onset potential of the HER which shifts towards more

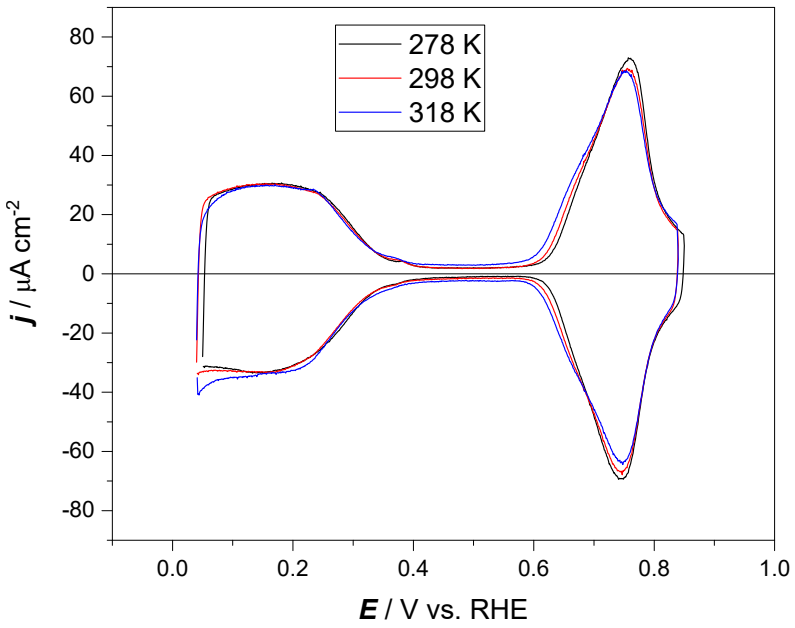

Figure 1: Cyclic voltammetries of Pt(111) at a scan rate of $50\,mV\,s^{-1}$ in 0.05 M NaOH at different temperatures.

positive values when the temperature is increased. Changes in the double layer region, between 0.4 and 0.6 V are negligible. Between 0.6 and 0.8 V, the current is attributed to OH^- adsorption. In this region, the half wave current density starts to increase with the temperature, but the actual current peak between 0.7 and 0.8 decreases. Since the main interest of this study is the hydrogen adsorption reaction, the working potentials for the impedance measurements were selected mainly in the low potential range, namely 0.045, 0.095, 0.145, 0.195, 0.245, 0.305, 0.345, 0.445 and 0.545 V. The last two selected potentials are outside of the hydrogen adsorption region. After a prolonged set of measurements, a small peak around 0.55 V signaled the accumulation of an unknown contaminant on the surface of the electrode. It is known that traces of Fe, Ni or Co ions in the solution lead to peaks in this potential range.[41] These contaminant species could be already present in the NaOH solid used to prepare the solution or come from the attack on the glass by the alkaline solution. However, the charge associated to this process remains below 0.75 $\mu C\,cm^{-2}$ after at least 10 minutes. For this reason, after every three EIS spectra collected at three different potentials, the electrode was flame annealed to eliminate this surface contamination.

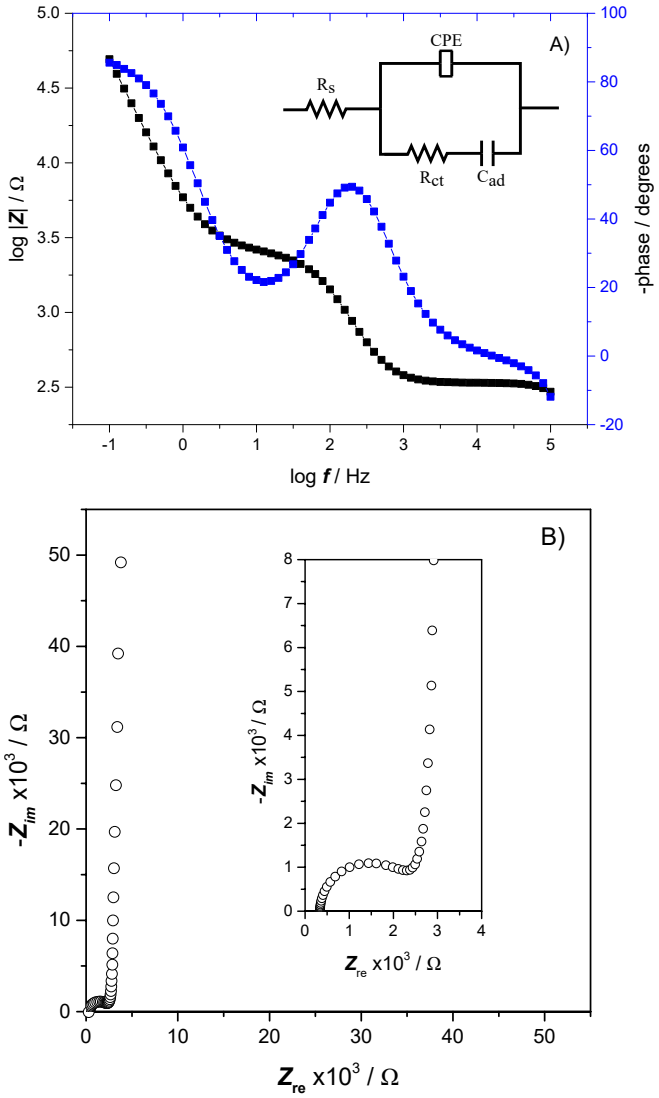

Figure 2: A) Logarithm of the absolute impedance and negative of the phase angle with respect to the logarithm of the frequency (Inset: equivalent electrical circuit) and B) impedance Nyquist plot with fit to the equivalent circuit, 25 °C at 0.145 V.

In figure 2, a typical Bode plot is shown (A) next to an admittance plot (B). Both measurements are typical and agree with the expected simulations of the equivalent circuit in the inset of figure 2.[42] The peak in the phase angle plot at high frequencies corresponds to the coupling of R_{ct} with C_{dl} and then it goes to -90 at lower frequencies when the admittance goes to 0 (infinite impedance). It is worth noting that this behavior is typical of a circuit with C_{dl} as an ideal capacitor. The radius of the low impedance semicircle in figure 2B corresponds to the inverse of the sum of solution and charge transfer resistance, but the characteristic shape of the Nyquist plots for impedance makes it difficult to obtain good fits. Therefore, the admittance plots were used to obtain the fitting curves to the equivalent circuit because the fitting gives more weight to the high frequency measurements.

In figure 3, the admittance Nyquist plots are shown. In such plots, the radius of the low-frequencies semicircle decreases when the potential increases at a constant temperature. This trend is signaling an increase in the charge transfer resistance with the potential. This semicircle is not present at the plot corresponding to the two highest potentials measured since the hydrogen adsorption does not occur in those cases. The opposite effect on this semicircle is observed with the increase of the temperature in figure 3B, where the radius is increasing with the temperature at a constant potential. In this case, both the resistance of the solution and the charge transfer resistance gets lower. This effect is more pronounced at the two highest temperatures. At a fixed potential, the influence of temperature on the different parameters of the equivalent circuit is shown on table 1.

Both resistances are affected by the change of temperature while the capacitance values remain approximately equal. The value of λ, which is the exponent of the frequency for the impedance of the constant phase element is approximately equal to unity, which was expected from the qualitative observation of the Bode plots. The value of λ has been attributed to be an indicator of the roughness of the surface, having a lower value when the surface has a greater number of defects.[43] The highly ordered plane of the Pt(111) surface is then expected to give the obtained value for this exponent, close to 1. Moreover, this would indicate that

Table 1: Fit parameters for the equivalent circuit at different temperatures and at $E = 145\,mV$

$T\,(K)$	$R_s\ (\Omega\,cm^2)$	$R_{ct}\ (\Omega\,cm^2)$	$Q/C_{dl}\,(mF\,cm^{-2})$	$C_{ad}\,(mF\,cm^{-2})$	$\lambda \pm 0.01$
278	24 ±6	190 ±42	21 ±1	0.54 ±0.02	0.99
283	24 ±4	208 ±41	21 ±2	0.53 ±0.05	0.99
288	20 ±4	153 ±15	21.8 ±0.8	0.53 ±0.03	0.99
293	20 ±4	151 ±6	21.2 ±0.5	0.55 ±0.01	0.99
298	17.4 ±0.5	127 ±16	21.7 ±0.9	0.54 ±0.01	0.99
303	18 ±2	114 ±16	22.2 ±0.9	0.54 ±0.01	0.99
308	16 ±4	94.7 ±32	22 ±2	0.54 ±0.01	0.99
313	13.28 ±0.07	42 ±14	25 ±2	0.54 ±0.02	0.98
318	13.0 ±0.4	36 ±3	23.9 ±0.9	0.55 ±0.01	0.99

the value Q must be a good estimation for the value for the capacitance of the double layer and it is similar to the values reported in previous works.[44,45]

The R_{ct} data obtained from the fittings was then plotted against the applied potential and the logarithm of the same value was plotted with respect to the inverse of the temperature to initially check for an Arrhenius type behavior. The results are shown in figure S1. The points corresponding to the two highest potential values deviate from the tendency of the other points because there is no hydrogen adsorption in this potential range. For the rest of the data points an exponential tendency can be seen. An approximate linear tendency is apparent in figure S1B, which indicates a linear relation with the standard rate constant k^0. Assuming a Frumkin type isotherm, the kinetic model describing the relation between R_{ct} and k^0 is given in equation (4) (the complete deduction of this expression is found in the supporting information):

$$R_{ct} = \frac{1}{q_{ML} f k^0 (1-\theta)^{1-\beta} \left(\frac{c_{OH^-}}{c^0}\right)^{\beta} \theta^{\beta} exp\left[g\theta\,(\beta-\alpha)\right]} \tag{4}$$

Here, q_{ML} is the charge of a monolayer on Pt(111) ($241\mu C\,cm^{-2}$), $f = F/RT$, θ is the surface coverage coefficient, β is the charge transfer coefficient, C_{OH^-} is the bulk hydroxyl concentration, c^0 is the standard state concentration 1 $mol\,L^{-1}$, g is the lateral interaction factor (Frumkin parameter) for adsorbed hydrogen and α is the charge transfer coefficient of

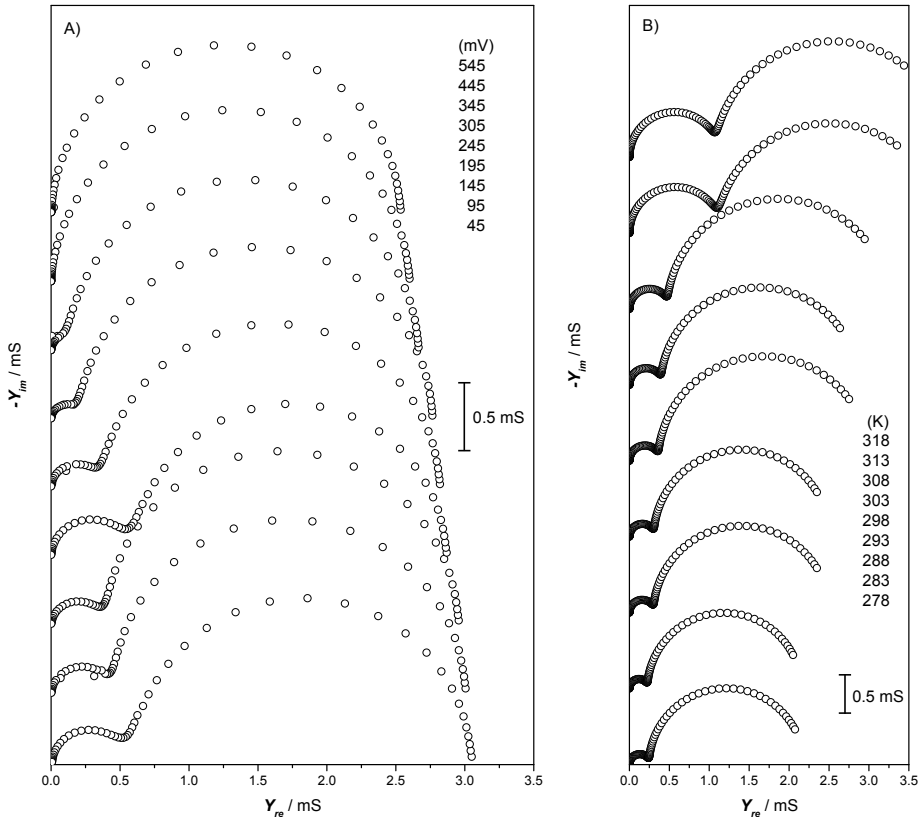

Figure 3: Nyquist plots of the admittance of Pt(111) on 0.05 M NaOH at (A) 25 $^{\circ}C$ with different potentials and at (B) 0.145 V with different temperatures.

the adsorption reaction. The charge transfer coefficient can be assumed to be approximately equal to the symmetry coefficient $\beta = \alpha = 0.5$ for a simple one electron transfer reaction, which then simplifies equation (4) to account for the most measurable and known information. The surface coverage can be calculated from the cyclic voltammetries at different temperatures. This is achieved by calculating the average current density of the hydrogen adsorption and desorption process (from ≈0.05 to ≈0.4 V) after subtracting the average current density associated with the double layer charge, measured as the average current between ≈0.45 and ≈0.55 V. The current density was then integrated with respect to the applied potential over the respective range, assuming that the maximum coverage is obtained with the charge that corresponds to q_{ML}, the result is a direct dependence of θ with respect to the applied potential and can be used in equation (4). This makes it possible to fit equation (4) to the data from figure 3A to obtain the value for the standard rate constant. The fits were obtained excluding the last two data points, that are outside the hydrogen adsorption region, and the results are shown in figure 4A, where the error bars were calculated using the standard deviation of the results. At higher potentials the charge transfer resistance increases, resulting in a smaller semicircle as can be seen in figure 3, thus there are less data points which in turn results in a higher error. This error is however not enough to significantly modify the overall result. A two-parameter non-linear fit was also done to evaluate the possibility of β being different from 0.5, but the results were indistinguishable. The k^0 values were then plotted against the inverse of the temperature in figure 4B.

From this plot an activation energy of $32\,kJ\,mol^{-1}$ can be calculated from the slope. An analysis to account for the entropy of activation of the reaction could be made using Eyring's equation, the difference is however small enough to fall within the error of the measurement. This value can then be used to compare with the results obtained by theoretical calculations. Hydrogen is thought to be adsorbed in two different thermodynamic states, H_{UPD} for potentials that are positive with respect to the RHE and H_{OPD} for negative potentials with respect to the same reference.[46] The H_{OPD} is difficult to measure electrochemically

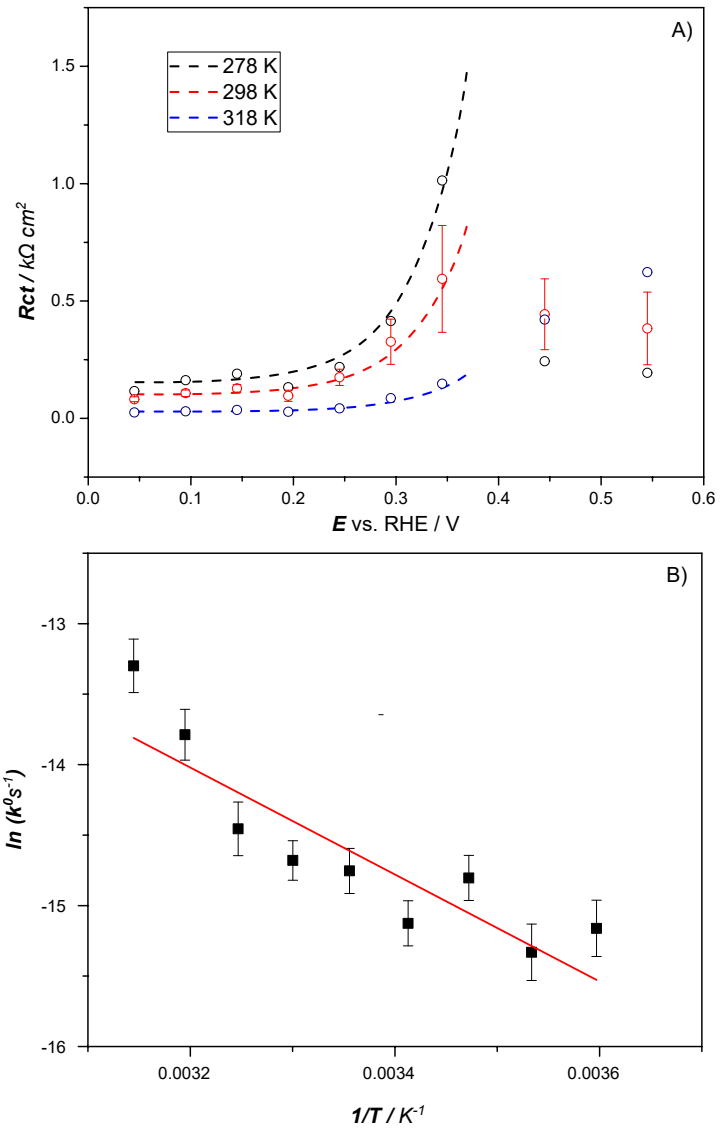

Figure 4: A) Fitted models of the charge transfer resistance with respect to applied potential (dashed) with experimental data points and B) rate constant with respect to the inverse of the temperature with Arrhenius type fit.

for Pt(111) since the HER occurs at the same potentials, but Conway et al.[47] interpreted that this species was the only one involved in the kinetics for the HER and the coverage on the electrode by H_{UPD} species of the electrode should favor the HER. The difficulties of the electrochemical measurements are "avoided" by computational simulations in which an analysis can be made without hydrogen evolution and specifying the different sites in which hydrogen can be adsorbed. Osawa et al.[48] used SEIRAS to observe that the adsorption of hydrogen on atop sites is energetically favored when there is a full monolayer (ML) of hydrogen already adsorbed, which means that H_{UPD} is adsorbed in hollow fcc sites and H_{OPD} binds to atop sites. Liu et al.[49] obtained comprehensive results showing that at potentials positive to the RHE potential there is a small presence of H atop, although the vast majority is adsorbed at hollow sites, but the presence of 0.006 ML of H atop increases the current density by a factor of 100. Skúlason et al.[50,51] calculated activation energies for the different steps leading to the HER and obtained a value of $42\,kJ\,mol^{-1}$ for the Volmer step, which is almost identical to the one obtained later by Jonsson et al.[52] This value is obtained assuming that the change of energy between solvated and chemically adsorbed hydrogen is zero and it is calculated based on proton concentration model. However, Morikawa[53] calculated this energy to be non-zero for hydrogen in fcc hollow sites and dependent on the added effect of the electric field, the solvent and the coverage on the surface. Considering that proton adsorption comes from water in alkaline media, changing the mechanism to the one studied by Skúlason, the calculated activation energy might be lower than the one obtained from the computational simulations due to a more stable Pt−H bond,[54,55] in agreement with the experimentally measured value in this work.

3.1 Conclusions

The temperature analysis shown here is proven to be a very suitable way to study the kinetics of hydrogen adsorption on Pt(111). The presented model allows to relate the charge transfer resistance with the standard rate constant, opening access to the activation energy for the

hydrogen adsorption, which turned out to be approximately $32\,kJ\,mol^{-1}$. This value is in good agreement with the ones obtained with DFT calculations for the Volmer step. A small discrepancy could be due to experimental conditions such as pH and solvent nature that are difficult to fully account for in a simulation. Further studies including the use of other Pt(hkl) basal planes and stepped surfaces will be carried out to gain fundamental insight for the influence of the surface structure on the reaction rate and the interactions of the absorbed molecules. Such systems might include further complications like the overlapping of the adsorption potential regions for OH^- and H^+ species, which could be overcome by a modified Frumkin isotherm. The accumulated experimental kinetic information on the hydrogen adsorption not only contributes to better understand the catalysis of hydrogen reactions but also supplies reliable data measured using state of the art methodologies to compare or validate a fast growing number of more and more refined theoretical calculations.

Supporting Information Available

The following files are available free of charge.

- SI.docx: The complete deduction of the mathematical relation between R_{ct} and k^0, the equation for the equivalent electrical circuit, datasets obtained from the non-linear fits to the impedance data and a graph with the initial apparent tendency of R_{ct} with the inverse of temperature.

Acknowledgement

This work has been financially supported by the MINECO (Spain) project No. CTQ2016-76221-P. L.E.B. thanks the Generalitat Valenciana for funding from the Santiago Grisolia Program (GRISOLIAP/2017/181).

References

(1) Gasteiger, H. A.; Markovic, N. M. Just a Dream or Future Reality? *Science* **2009**, *324*, 48–49.

(2) Kelly, N. A.; Gibson, T. L.; Cai, M.; Spearot, J. A.; Ouwerkerk, D. B. Development of a Renewable Hydrogen Economy: Optimization of Existing Technologies. *International Journal of Hydrogen Energy* **2010**, *35*, 892 – 899.

(3) Bockris, J. The Origin of Ideas on a Hydrogen Economy and its Solution to the Decay of the Environment. *International Journal of Hydrogen Energy* **2002**, *27*, 731–740.

(4) Roger, I.; Shipman, M. A.; Symes, M. D. Earth-Abundant Catalysts for Electrochemical and Photoelectrochemical Water Splitting. *Nature Reviews Chemistry* **2017**, *1*, 0003.

(5) Abe, J.; Popoola, A.; Ajenifuja, E.; Popoola, O. Hydrogen Energy, Economy and Storage: Review and Recommendation. *International Journal of Hydrogen Energy* **2019**, *44*, 15072–15086.

(6) Schmickler, W.; Santos, E. *Interfacial Electrochemistry*; Springer Berlin Heidelberg: Berlin, Heidelberg, 2010; pp 163–175.

(7) Greeley, J.; Jaramillo, T. F.; Bonde, J.; Chorkendorff, I.; Nørskov, J. K. Computational High-Throughput Screening of Electrocatalytic Materials for Hydrogen Evolution. *Nature Materials* **2006**, *5*, 909–913.

(8) Danilovic, N.; Subbaraman, R.; Strmcnik, D.; Chang, K.-C.; Paulikas, A. P.; Stamenkovic, V. R.; Markovic, N. M. Enhancing the Alkaline Hydrogen Evolution Reaction Activity through the Bifunctionality of $Ni(OH)_2$ Metal Catalysts. *Angewandte Chemie International Edition* **2012**, *51*, 12495–12498.

(9) Subbaraman, R.; Tripkovic, D.; Strmcnik, D.; Chang, K. C.; Uchimura, M.; Paulikas, A. P.; Stamenkovic, V.; Markovic, N. M. Enhancing Hydrogen Evolution

Activity in Water Splitting by Tailoring Li^+−$Ni(OH)_2$−Pt Interfaces. *Science* **2011**, *334*, 1256–1260.

(10) Climent, V.; Feliu, J. M. Thirty Years of Platinum Single Crystal Electrochemistry. *Journal of Solid State Electrochemistry* **2011**, *15*, 1297–1315.

(11) Asiri, H. A.; Anderson, A. B. Using Gibbs Energies to Calculate the Pt(111) H_{upd} Cyclic Voltammogram. *The Journal of Physical Chemistry C* **2013**, *117*, 17509–17513.

(12) Sakong, S.; Naderian, M.; Mathew, K.; Hennig, R. G.; Grob, A. Density Functional Theory Study of the Electrochemical Interface Between a Pt Electrode and an Aqueous Electrolyte Using an Implicit Solvent Method. *Journal of Chemical Physics* **2015**, *142*, 234107.

(13) Koper, M. T. Blank Voltammetry of Hexagonal Surfaces of Pt-Group Metal Electrodes: Comparison to Density Functional Theory Calculations and Ultra-High Vacuum Experiments on Water Dissociation. *Electrochimica Acta* **2011**, *56*, 10645–10651.

(14) Gómez, R.; Orts, J. M.; Álvarez-Ruiz, B.; Feliu, J. M. Effect of Temperature on Hydrogen Adsorption on Pt(111), Pt(110), and Pt(100) Electrodes in 0.1 M $HClO_4$. *The Journal of Physical Chemistry B* **2004**, *108*, 228–238.

(15) Zolfaghari, A.; Jerkiewicz, G. Temperature-Dependent Research on Pt(111) and Pt(100) Electrodes in Aqueous H_2SO_4. *Journal of Electroanalytical Chemistry* **1999**, *467*, 177–185.

(16) Clavilier, J.; Armand, D.; Sun, S. G.; Petit, M. Electrochemical Adsorption Behaviour of Platinum Stepped Surfaces in Sulphuric Acid Solutions. *Journal of Electroanalytical Chemistry* **1986**, *205*, 267–277.

(17) Clavilier, J. The Role of Anion on the Electrochemical Behaviour of a {111} Platinum

Surface; an Unusual Splitting of the Voltammogram in the Hydrogen Region. *Journal of Electroanalytical Chemistry* **1979**, *107*, 211–216.

(18) Conway, B.; Bai, L. Determination of Adsorption of OPD H Species in the Cathodic Hydrogen Evolution Reaction at Pt in Relation to Electrocatalysis. *Journal of Electroanalytical Chemistry and Interfacial Electrochemistry* **1986**, *198*, 149–175.

(19) Gennero de Chialvo, M.; Chialvo, A. The Tafel-Heyrovsky Route in the Kinetic Mechanism of the Hydrogen Evolution Reaction. *Electrochemistry Communications* **1999**, *1*, 379–382.

(20) Marković, N. M.; Grgur, B. N.; Ross, P. N. Temperature-Dependent Hydrogen Electrochemistry on Platinum Low-Index Single-Crystal Surfaces in Acid Solutions. *Journal of Physical Chemistry B* **1997**, *101*, 5405–5413.

(21) Jerkiewicz, G. Electrochemical Hydrogen Adsorption and Absorption. Part 1: Underpotential Deposition of Hydrogen. *Electrocatalysis* **2010**, *1*, 179–199.

(22) Ershler, B. Investigation of Electrode Reactions by the Method of Charging-Curves and With the aid of Alternating Currents. *Discussions of the Faraday Society* **1947**, *1*, 269.

(23) Randles, J. E. B. Kinetics of Rapid Electrode Reactions. *Discussions of the Faraday Society* **1947**, *1*, 11.

(24) Frumkin, A. Hydrogen Overvoltage. *Discussions of the Faraday Society* **1947**, *1*, 57.

(25) Lasia, A. Mechanism and Kinetics of the Hydrogen Evolution Reaction. *International Journal of Hydrogen Energy* **2019**, *44*, 19484–19518.

(26) Bard, A. J.; Faulkner, L. R. *Electrochemical Methods: Fundamentals and Applications*, 2nd ed.; Wiley: New York, 2001.

(27) Harrington, D.; Conway, B. AC Impedance of Faradaic Reactions Involving Electrosorbed Intermediates—I. Kinetic Theory. *Electrochimica Acta* **1987**, *32*, 1703–1712.

(28) Morin, S.; Dumont, H.; Conway, B. E. Evaluation of the Effect of Two-Dimensional Geometry of Pt Single-Crystal Faces on the Kinetics of upd of H Using Impedance Spectroscopy. *Journal of Electroanalytical Chemistry* **1996**, *412*, 39–52.

(29) Marinković, N.; Marković, N.; Adžić, R. Hydrogen Adsorption on Single-Crystal Platinum Electrodes in Alkaline Solutions. *Journal of Electroanalytical Chemistry* **1992**, *330*, 433–452.

(30) Oelgeklaus, R.; Rose, J.; Baltruschat, H. On the Rate of Hydrogen and Iodine Adsorption on Polycrystalline Pt and Pt(111). *Journal of Electroanalytical Chemistry* **1994**, *376*, 127–133.

(31) Lim, C.; Pyun, S.-I.; Ju, J.-B. Impedance Analysis of Hydrogen Adsorption on Palladium in 0.1 M NaOH Solution. *Journal of Alloys and Compounds* **1991**, *176*, 97–103.

(32) Sibert, E.; Faure, R.; Durand, R. High Frequency Impedance Measurements on Pt(111) in Sulphuric and Perchloric Acids. *Journal of Electroanalytical Chemistry* **2001**, *515*, 71–81.

(33) Schouten, K. J.; Van Der Niet, M. J.; Koper, M. T. Impedance Spectroscopy of H and OH Adsorption on Stepped Single-Crystal Platinum Electrodes in Alkaline and Acidic Media. *Physical Chemistry Chemical Physics* **2010**, *12*, 15217–15224.

(34) Sarabia, F. J.; Sebastián-Pascual, P.; Koper, M. T.; Climent, V.; Feliu, J. M. Effect of the Interfacial Water Structure on the Hydrogen Evolution Reaction on Pt(111) Modified with Different Nickel Hydroxide Coverages in Alkaline Media. *ACS Applied Materials & Interfaces* **2019**, *11*, 613–623.

(35) Cai, Y.; Anderson, A. B. The Reversible Hydrogen Electrode: Potential-Dependent Activation Energies Over Platinum From Quantum Theory. *Journal of Physical Chemistry B* **2004**, *108*, 9829–9833.

(36) Zhao, M.; Anderson, A. B. Predicting Reaction Mechanisms and Potentials in Acid and Base from Self-Consistent Quantum Theory: H(ads) and OH(ads) Deposition on the Pt(111) Electrode. *Journal of Physical Chemistry Letters* **2016**, *7*, 711–714.

(37) Tomonari, M.; Sugino, O. DFT Calculation of Vibrational Frequency of Hydrogen Atoms on Pt Electrodes: Analysis of the Electric Field Dependence of the Pt-H Stretching Frequency. *Chemical Physics Letters* **2007**, *437*, 170–175.

(38) Yeh, K. Y.; Janik, M. J.; Maranas, J. K. Molecular Dynamics Simulations of an Electrified Water/Pt(111) Interface Using Point Charge Dissociative Water. *Electrochimica Acta* **2013**, *101*, 308–325.

(39) Vasile, M. J.; Enke, C. G. The Preparation and Thermodynamic Properties of a Palladium-Hydrogen Electrode. *Journal of the Electrochemical Society* **1965**, *112*, 865–870.

(40) Macdonald, J. R. LEVMW. 2013; `https://jrossmacdonald.com/levmlevmw/`.

(41) Sarabia, F. J.; Climent, V.; Feliu, J. M. Underpotential Deposition of Nickel on Platinum Single Crystal Electrodes. *Journal of Electroanalytical Chemistry* **2018**, *819*, 391–400.

(42) Lasia, A. *Electrochemical Impedance Spectroscopy and its Applications*; Springer New York: New York, NY, 2014.

(43) Pajkossy, T. Impedance Spectroscopy at Interfaces of Metals and Aqueous Solutions - Surface Roughness, CPE and Related Issues. *Solid State Ionics* **2005**, *176*, 1997–2003.

(44) Pajkossy, T.; Kolb, D. Double Layer Capacitance of Pt(111) Single Crystal Electrodes. *Electrochimica Acta* **2001**, *46*, 3063–3071.

(45) Garcia-Araez, N.; Climent, V.; Herrero, E.; Feliu, J. M.; Lipkowski, J. Thermodynamic

Approach to the Double Layer Capacity of a Pt(111) Electrode in Perchloric Acid Solutions. *Electrochimica Acta* **2006**, *51*, 3787–3793.

(46) Barber, J. H.; Conway, B. E. Structural Specificity of the Kinetics of the Hydrogen Evolution Reaction on the Low-Index Surfaces of Pt Single-Crystal Electrodes in 0.5 M dm-3 NaOH. *Journal of Electroanalytical Chemistry* **1999**, *461*, 80–89.

(47) Conway, B. E.; Jerkiewicz, G. Relation of Energies and Coverages of Underpotential and Overpotential Deposited H at Pt and Other Metals to the 'Volcano Curve' for Cathodic H2 Evolution Kinetics. *Electrochimica Acta* **2000**, *45*, 4075–4083.

(48) Kunimatsu, K.; Senzaki, T.; Samjeské, G.; Tsushima, M.; Osawa, M. Hydrogen Adsorption and Hydrogen Evolution Reaction on a Polycrystalline Pt Electrode Studied by Surface-Enhanced Infrared Absorption Spectroscopy. *Electrochimica Acta* **2007**, *52*, 5715–5724.

(49) Fang, Y.-H.; Wei, G.-F.; Liu, Z.-P. Catalytic Role of Minority Species and Minority Sites for Electrochemical Hydrogen Evolution on Metals: Surface Charging, Coverage, and Tafel Kinetics. *The Journal of Physical Chemistry C* **2013**, *117*, 7669–7680.

(50) Skúlason, E.; Karlberg, G. S.; Rossmeisl, J.; Bligaard, T.; Greeley, J.; Jónsson, H.; Nørskov, J. K. Density Functional Theory Calculations for the Hydrogen Evolution Reaction in an Electrochemical Double Layer on the Pt(111) Electrode. *Physical Chemistry Chemical Physics* **2007**, *9*, 3241–3250.

(51) Skúlason, E.; Tripkovic, V.; Björketun, M. E.; Gudmundsdóttir, S.; Karlberg, G.; Rossmeisl, J.; Bligaard, T.; Jónsson, H.; Nørskov, J. K. Modeling the Electrochemical Hydrogen Oxidation and Evolution Reactions on the Basis of Density Functional Theory Calculations. *Journal of Physical Chemistry C* **2010**, *114*, 18182–18197.

(52) Van Den Bossche, M.; Skúlason, E.; Rose-Petruck, C.; Jónsson, H. Assessment of

Constant-Potential Implicit Solvation Calculations of Electrochemical Energy Barriers for H_2 Evolution on Pt. *Journal of Physical Chemistry C* **2019**, *123*, 4116–4124.

(53) Hamada, I.; Morikawa, Y. Density-Functional Analysis of Hydrogen on Pt(111): Electric Field, Solvent, and Coverage Effects. *The Journal of Physical Chemistry C* **2008**, *112*, 10889–10898.

(54) Ramaker, D. E.; Roth, C. Nature of the Intermediate Binding Sites in Hydrogen Oxidation/Evolution over Pt in Alkaline and Acidic Media. *ChemElectroChem* **2015**, *2*, 1582–1594.

(55) Sheng, W.; Zhuang, Z.; Gao, M.; Zheng, J.; Chen, J. G.; Yan, Y. Correlating Hydrogen Oxidation and Evolution Activity on Platinum at Different pH With Measured Hydrogen Binding Energy. *Nature Communications* **2015**, 6–11.

Graphical TOC Entry